Reinterpretation of The DSC Data for Atactic Polystyrenes by Stadnicki et al.

RAYMOND F. BOYER, *Michigan Molecular Institute, 1910 W. St. Andrews Road, Midland, Michigan 48640*

Synopsis

Reexamination of published DSC traces for first and second heatings of atactic polystyrenes with $\overline{M}_n$ from 2050 to 1.99×10^6, $\overline{M}_w/\overline{M}_n \sim 1.1$, is discussed in terms of some newly enunciated principles of calorimetry for the liquid state of atactic polymers. These traces were originally stated to reveal only an endothermic peak above T_g, identified with T_{ll} at $\overline{M}_n <$ ca. 10^5. Three types of behavior are now distinguished: (1) First heating, $\overline{M}_n < M_c$ (the entanglement molecular weight), an endothermic slope change attributed to T_{ll}, followed by an exotherm at T_{exo} ascribed to melt flow and/or wetting of the DSC pan; (2) first heating for $\overline{M}_n$ above M_c, only an endothermic slope change; (3) second heating, all molecular weights, only an endothermic slope change for T_{ll} and, in some cases, $T_{l\rho}$. T_{ll} thus defined reaches an asymptotic limit when plotted against log $\overline{M}_n$, just as T_g does. Texo begins to level off, and then, starting at M_c, increases without limit. T_{ll} is an isofree volume state as is T_g; T_{exo} is an isoviscous state and hence a pure relaxation process. DSC traces on first heating at $\overline{M}_n < 10^5$ provide the first known experimental evidence for both the transitional and the relaxational aspects of T_{ll} in the same experiment. The role of zero shear melt viscosity, η_0, in DSC is noted: T_{ll} depends only on $\overline{M}_n$; T_{exo} on η_0 and hence on $\overline{M}_w$. The T_{ll} temperature is independent of physical form of the specimen: powder, pellet, film. DSC studies on bimodal blends of PS show T_{ll} uniquely dependent on $\overline{M}_n$, while the $T_f - (T_{exo})$ exotherm depends on $\overline{M}_w$. Such blends can eliminate interference between the T_{ll} endotherm and the T_f exotherm. Exotherms using weighted pan lids and exotherms from sintering are also presented. DSC evidence for $T_{l\rho} > T_{ll}$ is indicated.

INTRODUCTION

Stadnicki et al.[1,2] reported DSC observations on particulate PSs as a function of $\overline{M}_n$, using open DSC pans at a heating rate of 30 K min^{-1}. A molecular weight dependent endothermic peak was found with the peak becoming broader and less distinct as $\overline{M}_w$ approached 10^5. These peak temperatures, labeled T_{ll}, were shown to represent an isoviscous state with log η_0 (P) lying between 4 and 5 as shown in Figure 17 of Ref. 2. η_0 is the zero shear melt viscosity of the polymer in poise (P).

These endothermic peaks have been discussed before[3-5] with no totally conclusive idea of their origin. We do not view the present paper as an extension of that controversy since we start from a series of sequential studies in progress for over 2 years and originally with no regard to the Stadnicki data.

1. A comprehensive review of the literature on T_{ll} and related liquid state transitions and relaxations.[6]

2. Extension of the hot stage microscope investigation of PS[7] to include a theoretical background basis for the observed phenomena.[8,9*]

*Reference 8 is on the molecular basis of T_{gl} and T_f. The basic concepts are indicated in Refs. 10 and 11.

Journal of Applied Polymer Science, Vol. 33, 955–969 (1987)
 CCC 0021-8995/87/030955-15$04.00

3. Recognition of some new principles concerning the liquid state calorimetry of atactic polymers and copolymers.[10]

4. A study of published C_p–T data above T_g for acrylate, methacrylate, and hydrocarbon polymers by Wagers and the author[11] was made which confirmed these new principles. A method for estimating exothermic heats from viscous flow above T_g in the DSC cell was given.

5. A suggestion in Section 3.3 of Ref. 11 stated that the endothermic peaks observed by Stadnicki et al.[2] might represent a competition between an endothermic T_{ll} event and an exothermic viscous flow process.

6. A preliminary reexamination of the Stadnicki et al. DSC data confirmed the above suggestion with important consequences for T_{ll} and DSC. This is the subject of the present paper; but first a summary of the current status of our hot stage microscope studies is in order.

Hot stage microscopy of particulate at-PSs with $\overline{M}_w/\overline{M}_n \sim 1.1$ at a heating rate of 10 K min^{-1}[7-9] revealed two molecular weight dependent processes above T_g:

a. A sintering process resulting in the formation of one or more spherical globules of molten polymer at a temperature labeled T_{g1}.

b. A flow process starting at T_f with wetting of the glass substrate by the spherical globule(s) under the driving force of interfacial surface tension plus a gravity effect contributed by a cover glass resting on the polymer.

c. Keinath[9] has photographed compacted specimens of at-PS inside a DSC cell and obtained dimensions of the specimen as a function of T. Quantitative information about the T_{g1} and T_f processes is obtained, confirming the visual observations by hot stage microscopy, and consistent with DSC events.

The molecular weight dependence of T_{g1} and T_f is given in Figure 4 of Ref. 7(a) and in a different form as Figure 1 of Ref. 11, either of which shows $T_f > T_{g1} > T_g$ at all molecular weights. Both T_{g1} and T_f were recognized to be exothermic. The T_{g1} exotherm has been observed in DSC only under special circumstances discussed in 11 and in Appendix A. The T_f exotherm is much more important for our purposes.

Key molecular parameters affecting flow over a substrate were given by Schonhorn et al.[12] in the expression:

$$a_T = \gamma/\eta_0 L \tag{1}$$

where γ is surface tension dyn/cm, η_0 is zero shear viscosity, and L is a scaling factor (dimensions, cm), which is independent of temperature and molecular weight. a_T has the dimensions of s^{-1} and hence may be considered as a shear rate. For more general background on flow of molten polymer on substrates, see Wu[13], while Lau and Burns provide experimental data on at-PS.[14†] It is known (see Refs. 11 and also 16) that the dissipative energy associated with viscous flow is given by

$$E\ (\text{ergs/s cm}^3) = \eta_0(\dot{\gamma})^2 \tag{2}$$

† References 15(a) and (b) provide new measurements of equilibrium contact angles.

where γ is shear rate, considered in Ref. 11 to be a_T.‡ Hence;

$$E = \gamma^2/\eta_0 L^2 \tag{3}$$

We have shown (8) that for a heating rate of 10 K min^{-1} γ at T_f is 35 dyn/cm, η_0 at T_f is 3.5×10^5 P. L was estimated in Ref. 11 to be 10^{-4} cm. Thus E in units pertinent to DSC became

$$E \text{ (mJ/s 10 mg polymer)} = 1.225 \times 10^5/\eta_0 \tag{4}$$

an amount considered detectable at and above T_f by DSC.[11] This leads to a new prediction, stated here for the first time:

Whereas the exothermic flow process starts at T_f, it may not affect the DSC trace perceptibly until a temperature called T_{exo} is reached at $T_f + \Delta T$.

ΔT may depend somewhat on molecular weight, certainly on sensitivity setting of the DSC instrument, heating rate, and possibly other factors. ΔT increases without limit above M_c as a function of $\bar{M}_w$ as shown later in Figure 4. We have found for bimodal blends at constant $\bar{M}_n$ that ΔT increases with $\bar{M}_w/\bar{M}_n$ (see Appendix A).

The initial rate of isothermal spreading without gravity drops rapidly towards zero as spreading proceeds, according to a factor $(\cos\theta_i - \cos\theta_f)$ where θ_i is the initial, θ_f the final wetting angle, also designated θ_s, the static contact angle.[13-15] In the nonisothermal situation which prevails in DSC, eq. (3) term increases exponentially while the cosine term decreases even more rapidly. (See Refs. 12, 14, and 15 for details.) The net result should be a broad maximum in heat evolution which should occur above T_{exo}.

Note: The DSC results of Stadnicki[1,2] and our studies on hot stage microscopy[7,8] were conducted on anionically prepared PSs with $\bar{M}_w/\bar{M}_n \sim 1.05$. Likewise, the several parameters, γ, θ, and η_0, used in the above equation are available for anionic PSs as part of the general literature concerned with interface science and melt rheology. Values of γ and θ_s are found in Table II of Ref. 14(b), and more θ_s values in Ref. 15; η_0 values are widely scattered in the literature but Ref. 17 gives two specific sources which we have used. Table I of Ref. 17(b) lists sources of $\log \eta_0$ data at various molecular weights from 600 to 1.2×10^6. Experimental proof that the spreading of molten PS on glass is dominated by η_0 in eq. (1) at $M \leq M_c$ is found in Figure 2 of Ref. 14(b). We have shown[8] that γ at T_f is essentially constant at 35 dyn/cm, primarily because the increase in γ with $\bar{M}_n$ and the decrease in γ with T essentially cancel each other at T_f. With the above background on hot stage microscopy and exotherms attendant on flow, the DSC data of Stadnicki

‡Equation (2) was ascribed in Ref. 11 to our colleague, Dr. Dale Meier, who could not cite a literature reference. We subsequently found the identical equation employed in estimating a heat for sintering for PMMA by Rosenzweig and Narkis,[16] who also did not cite a source. [See their eq. (5) on p. 1168.]

et al. can be considered. New experiments results on PS supporting our reinterpretation of the Stadnicki data follows as Appendix A.

THE STADNICKI ET AL. DSC RESULTS

We examined photo enlargements of the original traces as given in Figure 5 of his thesis[1] but seen much reduced in the published Figure 5.[2] It was apparent that the traces were not only a function of thermal history but also of $\overline{M}_n$ on first heating. Figure 1 shows four first heating traces at, below, and above M_c. We identify T_{ll} as the start of the endothermic process, and T_{exo} as the peak which was previously designated as T_{ll} in Refs. 1 and 2. Second heating traces no longer show T_{exo} since the wetting and flow processes can only occur on the first heating unless the polymer film formed on the first heating is mechanically or thermally fractured. Over half of the second heating traces do show endothermic slope changes; others do not. Origin of the first-heating endotherms at $\overline{M}_n > M_c$ are treated in the Discussion section.

Table I collects our values of T_{ll} from first and second heatings as well as T_{exo} values formerly labeled as T_{ll}.[1,2]

Figure 2 plots these values of T_{ll} and T_{exo}, to emphasize the marked difference in character. T_{ll} has the classical behavior: remaining parallel to T_g with a sharp increase at first, followed by leveling off to an asymptotic limit with a limiting ratio of $T_{ll}/T_g \sim 1.17$. Such behavior is shown in Figure 1(B) and Figure 36 of Ref. 6.

The T_{exo} locus parallels T_f behavior, including the sharp slope increase above M_c seen in Figure 4 of Ref. 7. T_{exo} appears to increase without limit above M_c, as does T_f.

Only the upper locus appears in Figure 7 of Ref. 2 incorrectly labeled T_{ll}. The DSC data are supplemented by torsional braid analysis (TBA) points at ca. 0.3 Hz.[1,2] Contrary to our earlier view in Ref. 2, we now believe that the TBA method, involving oscillating shear, yields T_f at $M > M_c$ but T_{ll} values below M_c (see Fig. 36 of Ref. 6).

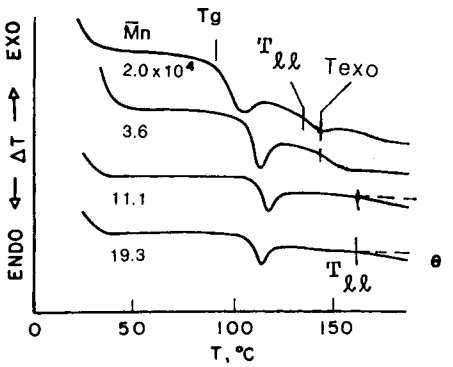

Fig. 1. Enlarged first heating DSC traces for at-PSs of indicated $\overline{M}_n$ values. T_{ll} marks the start of endotherm associated with the liquid–liquid transition. T_{exo} indicates the exotherm associated with a viscous flow process. The angle θ, expressed as radians per 100 mg, is used later to measure intensity of the T_{ll} process.

TABLE I
Summary of T_{ll} Values by DSC[a,b]

$\bar{M}_n$[c]	T_g (K)[c]	T_{ll} (K)[d]	T_{ll}/T_g[d]	T_{ll} (K)[e]	T_{ll}/T_g	T_{exo} (K)[f]
2050	343	361	1.05	364	1.06	363
3100	356	376	1.06	388	1.09	388
9600	362	395	1.09	—	—	407
20,400	365	407	1.12	409	1.12	416
36,000	378	417	1.10	415	1.10	431
111,000	385	435	1.13	—	—	475
193,000	381	429	1.13	—	—	—
355,000	384	—	—	432	1.13	—
640,000	385	453	1.18	—	—	—
1,990,000	383	—	—	443	1.16	—

[a] Heating rate, 30 K min^{-1}.
[b] Our values of T_{ll} defined in Figure 1.
[c] Table III, Ref. 2.
[d] First heating.
[e] Second heating.
[f] Same as column marked T_{ll} in Table III of Ref. 2.

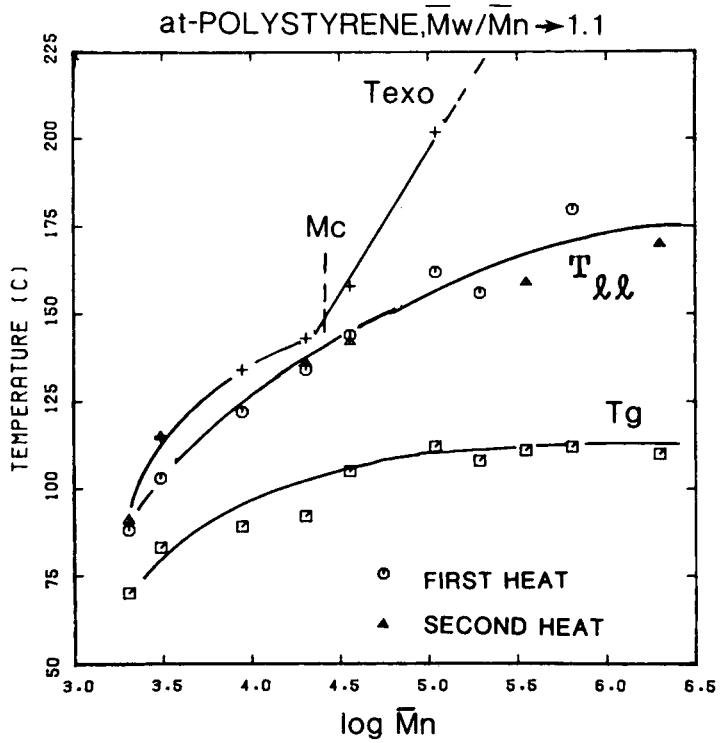

Fig. 2. Loci for T_g, T_{ll}, and T_{exo} defined in Figure 1 as a function of log $\bar{M}_n$. M_c is the entanglement molecular weight. T_g and T_{ll} are isofree volume states, T_{exo} an isoviscous state with log $\eta_0 = 4.5$ for the heating rate employed and with η_0 in poise. T_{exo} is from Refs. 1 and 2, as is T_g; T_{ll} is from the present study: (⊙) first heat; (▲) second heat.

DISCUSSION OF RESULTS

Table I and Figure 2 represent the first occasion known to us when the T_{ll} transition and the $T_f > T_g$ relaxation process have been observed as a function of molecular weight in the same experiment. Obviously this is possible only on the first heating.

We have long recognized[6] that $T_{ll} \sim 1.2\ T_g$ appears in physical methods which do not involve macroscopic flow of molten polymer, i.e., volume–temperature, volume–pressure, C_p–T, and η_0–T. Conversely, test methods involving shear such as the torsion pendelum, or penetrometry, and flow tests in general, give rise to the isoviscous T_f relaxation above M_c, whose temperature depends on the time scale of the experiment.

Hence, it follows that both conditions exist in the DSC cell under suitable circumstances. In the present case these conditions appear in sequence. It is readily apparent from Figure 2 why the first heating traces of Figure 1 change character so abruptly above M_c. As T_{ll} levels off and T_{exo} rises, there can be no interference with the T_{ll} endotherm except at high temperatures. T_{ll} is observed without complications.

With regard to second heating traces, fusion and flow have been accomplished (except perhaps at high values of $\overline{M}w$). Hence, one should detect only endotherms on second heating, as was observed by Enns et al.[18] It is not clear why some traces fail to show an endotherm but sample weight could be responsible. Some traces, notably $\overline{M}_n = 9600$, show an exotherm on both first and second heatings. The latter is not understood.

We also stress the implication of a simple fact: When endotherms occur on the first and second heatings, they give essentially identical values of T_{ll}. The physical form of the specimen is quite different during first and second heatings as well as below and above M_c on the first heating. Three situations can be distinguished:

1. During second heating, the specimen is a coherent film in good contact with the DSC pan.

2. Below M_c during the first heating, the specimen experiences a physical transformation from loose powder with low thermal conductivity and poor contact with the DSC pan to spherical molten globules to a spreading film of molten polymer which wets the DSC pan.

3. Above M_c during first heating, the specimen remains a loose powder through T_{ll} until the temperature reaches T_{gl} and/or T_f.

We, therefore, conclude that the endothermic event associated with T_{ll} is independent of physical form of the specimen at least in the data of Ref. 2. It also follows that T_{ll} is not dependent on the change in physical form and/or thermal conductivity which occurs during first heating as we once believed (p. 57 of Ref. 7). This statement refers to PS specimen weights of ca. 5 mg or less.

These several conclusions can be illustrated by a specific experiment. A ca. 10 mg pellet of PS obtained by fracturing a compression-molded PS plate ($\overline{M}_n = 37{,}000$) was placed in an open Teflon-coated DSC plan and heated at 10 K min^{-1} to 200 °C. When the DSC cell was opened for visual inspection at 200 °C, the pellet, originally of irregular shape, appeared as a spherical globule, presumably formed at $T_{gl} < T_{ll}$ and preserved as a sphere by surface tension. The specimen was recovered as a hard sphere on cooling to ca. 20 °C.

A strong endotherm at T_{ll} was observed during the first heating cycle. This experiment confirmed our conclusion that T_{ll} is not associated with the wetting process.

We do, of course, recognize that there can be endotherms other than those resulting from T_{ll}, such as loss of volatiles from an open DSC pan.[3] But we have shown in Figures 3 and 4 of Ref. 4 that added volatile matter behaves differently than T_{ll} on first heating and that its manifestation is absent on a second heating, while the T_{ll} endotherm remains.

The other key aspect of T_{ll} is its intensity, defined in Figure 1 as radians per unit weight. Since specimens weights are not known, comparisons can not be made as a function of $\overline{M}_n$ on first heating. For each $\overline{M}_n$, specimen weight is presumed to be very similar for first and second heatings. Intensity appears to be less on second heating, which could be a result of physical form or destruction of nascent morphology on first heating through T_{ll}.

The results of our current analysis are consistent with the DSC finding of Enns et al.[18-20] They made the empirical observation that T_{ll} could be observed in at-PSs as a function of $\overline{M}_n$ from 2200 to 2×10^6 by a four-step procedure: (a) first heating the particulated PS in an open DSC pan to 200 °C; (b) holding at 200 °C for ca. 10 min; (c) slow cooling to RT; and (d) reheating at 40 K min^{-1}.

The rationale for this empirical procedure became apparent only recently: The first heating not only removed atmospheric O_2, H_2O, and residual monomer but also achieved fusion and flow so that there should be no exotherm(s) interfering with T_{ll} on any subsequent heating.

Enns was also able to locate $T_{l\rho} > T_{ll}$ as a second endothermic slope change, not only in at-PSs but in numerous other atactic polymers.[18(b)] The current status of $T_{l\rho}$ is reviewed on pp. 308ff of Ref. 6. It is considered to be intramolecular and arising from barriers to rotation about main chain bonds, in contrast to T_{ll} which is considered to be of intermolecular origin (pp. 251ff of Ref. 6).

Finally, we reconsider the DSC data of Kokta et al.[21] on the same series of PSs used by Stadnicki but in hermetically sealed DSC pans at heating rates of 10 and 20 K min^{-1}. Their data are displayed as C_p–T plots which show an $\overline{M}_n$-dependent endothermic peak in C_p above T_g. They identify these peaks with T_{ll}.

The small scale of their C_p–T plots and the absence of tabulated data preclude an accurate reanalysis of their results similar to that reported here. They did not show C_p–T plots in the decisive $\overline{M}_n$ region from below, through, and then above M_c. Qualitatively, their findings are not inconsistent with conclusions herein.

Since Enns et al.[18-20] showed that T_{ll} could be located with certainty at all values of $\overline{M}_n$ for at-PS on a second heating, and since many DSC investigators prefer to discard first heating results in favor of a second heating, one might conclude that there should never be a problem. Our concern is broader, however, and includes:

1. A basic understanding of DSC data such as the ones presented by Stadnicki et al.[1,2], by Kokta et al.,[21] and by others. For example, DSC traces on polymethacrylates by Lai[22] show endothermic peaks. Tabulated DSC data on PS by Bares and Wunderlich reveal an endothermic maximum[23]; even

tabulated adiabatic calorimeter data on at-PS by Karasz et al.[24] has been found by us to exhibit an endothermic peak (see Fig. 25C of Ref. 6). Since $\bar{M}_n \gg M_c$ and $\bar{M}_w/\bar{M}_n \sim 2$, we ascribe the endothermic peak in Ref. 24 to a sintering exotherm occurring above T_{ll}, as would be predicated by Figure 1 of Ref. 11.

2. It is our belief that nascent short range structure present in a specific polymer because of prior history may be destroyed during first heating. It has been shown that an intense T_{ll} induced in at-PS by pressurization above T_{ll} followed by cooling under pressure is found only on first heating in a DSC cell, but is absent on second heating (Fig. 35 of Ref. 6).

3. The Enns et al. second heating method has the advantage of revealing not only T_{ll} but also the intramolecular $T_{l\rho} > T_{ll}$ process in PS and in a number of other polymers.[19] For current details about $T_{l\rho}$, see Figure 1(B) and Tables I and XI of Ref. 6.

We end by restating a general principle proposed in Ref. 10 and demonstrated in Ref. 11: that polymers with T_f well below room temperature are liquid when placed in the DSC cell or calorimeter. Exotherms associated with fusion and flow are complete before the calorimeter run begins. Calorimetry on these low T_f polymers has consistently revealed an endotherm at T_{ll} on first heating.[10] This is not a molecular weight effect as shown in Table II of Ref. 11. Conversely, polymers with T_f well above room temperature tend to show at least one exotherm on first heating (see Table I of Ref. 11).

SUMMARY AND CONCLUSIONS

1. The DSC traces of Stadnicki et al.[2] contains more and different information than was originally stated.

2. First and second heatings show evidence (with a few exceptions) for T_{ll} as an endothermic slope changes. These T_{ll} values meet general criteria for T_{ll},[6] i.e., reaching an asymptotic limit at high $\bar{M}_n$ with $T_{ll}(\infty)/T_g(\infty) \rightarrow 1.20 \pm 0.05$, where ∞ signifies a limiting high molecular weight value of T_g and T_{ll}.

3. The endothermic peak labeled in Ref. 2 as T_{ll} is now considered to signify the start of a detectable exotherm associated with viscous flow, and labeled here for the first time as T_{exo}. T_{exo} is $T_f + \Delta T$, where T_f is the flow temperature from hot stage microscopy and ΔT may depend on heating rate.

4. Calorimetry of the liquid state of atactic polymers is more involved than that for T_g because of the possibility of a succession of alternating endotherms and exotherms, namely, endo at T_g exo at T_{gl}, endo at T_{ll}, exo at T_{exo}, and an endotherm at $T_{l\rho}$.

5. These alternations in endo-exo may be responsible for the practice of representing C_p above T_g as linear in T.[11]

6. The earlier speculation of Wagers and the writer[11] about the Stadnicki endotherm peaks is not only confirmed but amplified. Moreover, a qualitatively similar conclusion is possible using the DSC data of Kokta et al.[21]

7. It is demonstrated by DSC first heating experiments on bimodal blends of PS that the separation between T_{ll} and T_{exo} along the temperature scale can be controlled at will by choosing $\bar{M}_w \gg \bar{M}_n$ for $\bar{M}_n < M_c$. This leads to an unambiguous location of T_{ll} (see Appendix A).

8. The finding by Enns et al.[18-20] that second heatings reveal T_{ll} and $T_{l\rho}$ without interference from exotherms is confirmed (see Appendix A).

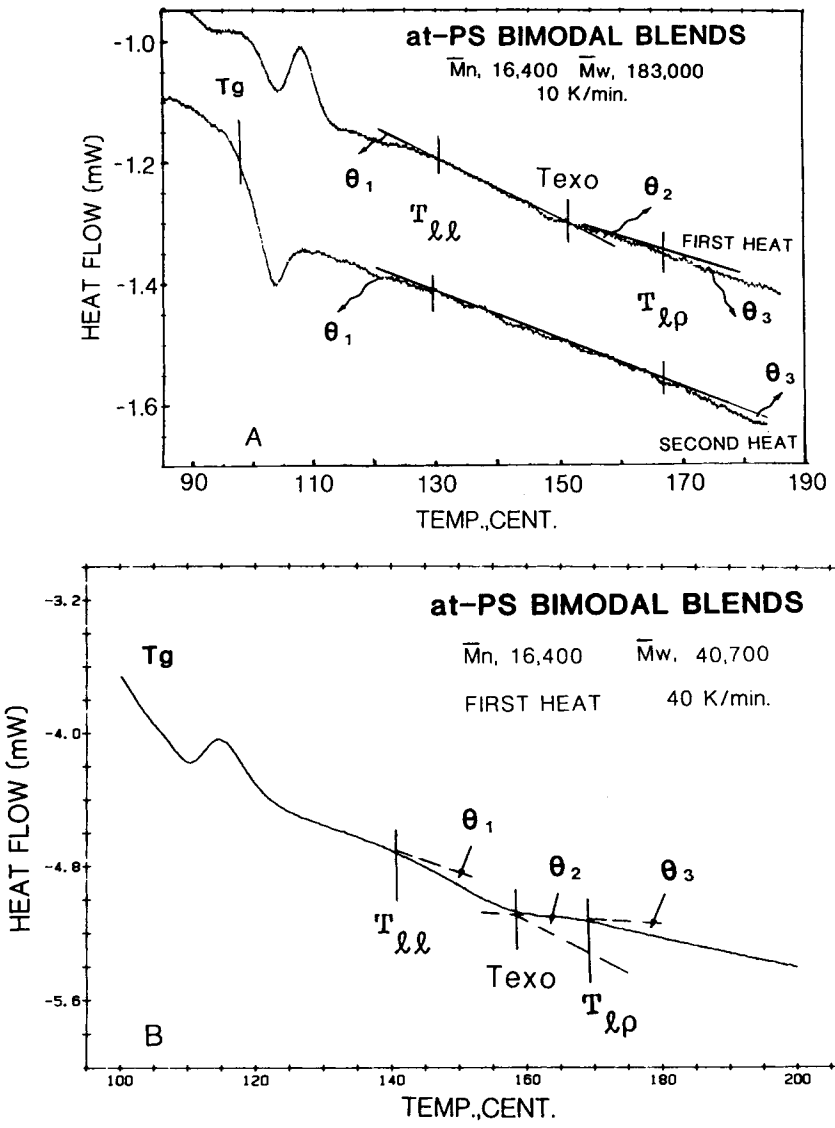

Fig. 3. (A) First and second DSC heating traces on the indicated bimodal blend of at-PS at 10 K/min with construction lines to indicate slope changes at the several transitions. (B) First heating only at 40 K/min. Angles θ_1, θ_2, and θ_3 are collected in Table II; T_{ll} and T_{exo} are given in Figure 4.

9. It is shown in Figure 4, for the first time using DSC data, that T_{ll} depends uniquely on $\bar{M}_n$, at least for the specific bimodal blends employed. This $\bar{M}_n$ dependence is believed to be general.

This material was first presented in a rudimentary form as part of a lecture on liquid state calorimetry at the Princeton University Polymer Seminar on October 11, 1984. The ensuing discussion was most helpful. We wish to recognize belatedly a conversation with Professor Thomas Lloyd, Department of Chemistry, Lehigh University in the fall of 1984. He mentioned microcalorimeter experiments which indicated detectable heat from viscous flow of polymer solutions. This resulted indirectly in eq. (A-2) of Ref. 11 and eq. (3) of the present report. The role

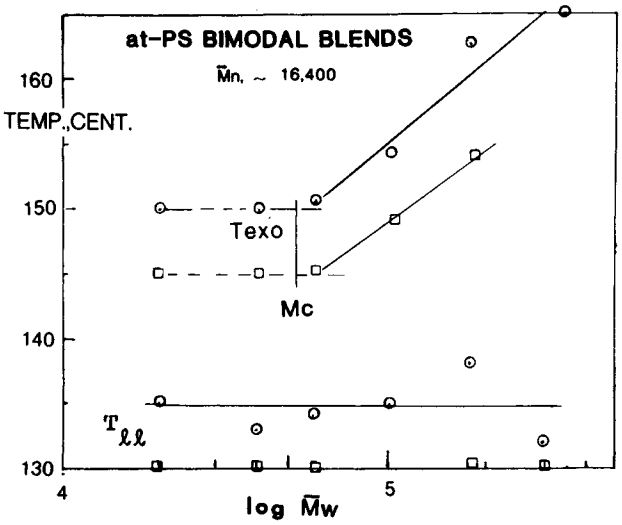

Fig. 4. T_{ll} and T_{exo} as a function of $\bar{M}_w$ for bimodal blends of at-PS with $\bar{M}_n$ ranging from 15,000 to 17,950 at two heating rates. [(○) 40 K/min; (□) 10 K/min]. Average value of $\bar{M}_n$ is 16,400.

of Dr. Dale Meier, MMI, in eq. (3) is discussed in Ref. 16. Mrs. Mary L. Wagers, formerly of MMI, carried out, at our suggestion, the several experiments described in Appendix A. We are indebted to Professor M. Narkis, Technion, Haifa, Israel, who supplied a set of his publications on sintering, and to Professor Richard Wool, University of Illinois, Champaign-Urbana, Illinois, who recommended that we try to locate publications by Professor Narkis. Professor Charles Burns, University of Waterloo, sent us reprints of Ref. 15. Comments by two reviewers resulted in clarifying changes at several places in the manuscript. Finally, we wish to state that no criticism of Stadnicki[1] or of Kokta et al.[21] is intended. Too little was known then about the nature of T_{ll} and the many aspects of T_{ll} to reach any other conclusions. The calorimetric principle contingent on understanding T_{ll} had not been enunciated. As a co-author of Ref. 2 we certainly agreed with all conclusions reached in that paper. Only much later did we reverse our perspective and definitions.[6] An overall appreciation of the contributions of Gillham and his students to T_{ll}, using both torsional braid analysis and DSC, appears on p. 250 of Ref. 6, with particular emphasis on results obtained for $\bar{M}_n < M_c$.

APPENDIX A: SUPPORTING EXPERIMENTAL EVIDENCE FROM BIMODAL BLENDS OF PS

DSC of Bimodal Blends of PS

It was evident from Figure 1 and 2 that the temperature interval, $T_{exo} - T_{ll}$, tended toward zero with decreasing $\bar{M}_n$. One possible means to avoid this dilemma is to utilize the principle that T_{ll} depends on $\bar{M}_n$ while melt flow, as in the hot stage microscope experiments,[7,8] and in DSC depends on $\bar{M}_w$.

The first experimental demonstration that T_{ll} depends on $\bar{M}_n$ was reported by Glandt et al.[25] using bimodal blends of narrow distribution PSs measured by torsional braid analysis (shear) below M_c. Keinath and the writer extended these observations with deformation in flexure,[26] again for bimodal blends of PS. The present study extends these results to DSC.

The η_0 dependence of flow and attendant exotherms, as apparent in eqs. (1)–(4), suggested DSC experiments on bimodal blends of PS as a means of separating the endothermic T_{ll} process from the exotherm associated with flow and wetting. Bimodal blends with constant $\bar{M}_n < M_c$ and $\bar{M}_w \gtrless M_c$ were prepared in chloroform (~ 1 wt% PS), allowed to age at RT for at least 7 days, and precipitated in methanol. The precipitates were dried, pelletized, ground in a mortar and pestle, and measured at 10 and 40 K min^{-1} using the duPont 1090-920 DSC system.[27]

TABLE II
Summary of DSC Results for Bimodal PS Blends, Constant $\overline{M}_n$ Intensities of Endotherms θ_1 and θ_3 and Exotherm θ_2 (rad/100 mg)[a]

			A: 10 K/min, Al pans first and second heatings				B: 10 K/min, Teflon-coated pans, first heating				C: 40 K/min, Al pans and Teflon-coated pans, first heating			
				Intensities[c,d]				Intensities				Intensities[c,e,f]		
Blend no.	$\overline{M}_n$[b]	$\overline{M}_w$[b]	Sample wt (mg)	θ_1	$-\theta_2$	θ_3	Sample wt (mg)	θ_1	$-\theta_2$	θ_3	Sample wt (mg)	θ_1	$-\theta_2$	θ_3
1	15.1	20.4	5.15	4.4	4.0	—	5.09	7.9	4.8	0.0	5.09	2.7	7.2	1.4
				(1.4)	(0.0)	—					(5.09)	(3.4)	(5.1)	(1.7)
2	15.3	40.7	4.50	8.1	8.9	3.8	5.04	2.9	3.8	0.0	5.04	3.1	5.2	—
				(1.9)	(0.0)	(—)					(5.17)	(2.4)	(6.4)	(3.0)
3	15.4	61.0	4.27	5.7	9.4	—	5.18	4.4	5.1	1.7	5.15	2.4	5.2	0.0
				(0.0)	(0.0)	—					(5.19)	(3.4)	(6.1)	(—)
4	15.7	102	4.29	4.1	5.7	—	5.09	3.8	6.9	1.4	5.18	2.0	4.7	0.0
				(1.6)	(0)	—					(5.21)	(3.0)	(6.7)	(0.0)
5	16.4	183	4.01	5.7	6.5	—	5.11	4.4	3.8	1.4	5.20	2.2	5.5	0.0
				(3.7)	(0.0)	(6)					(5.11)	(1.4)	(2.7)	(0.0)
6	18.0	345	4.86	[g]	[g]	[g]	5.19	5.0	[g]	[g]	5.14	2.0	6.8	0.0
				(—)[g]	(—)[g]	(—)[g]					(5.18)	(1.3)	(6.7)	(—)
	Average 1st heating			5.60	6.90	—		5.51	4.88[h]		Average	2.40[i]	5.77[i]	—
												(2.48)[d]	5.61[d]	(—)

[a] Angles defined in Figures 3(A) and (B).

[b] Blends were based on component A, M_n = 15,100 and $\overline{M}_w$ = 20,400, and component B, $\overline{M}_n = 1.99 \times 10^6$, $\overline{M}_w = 2.05 \times 10^6$ with the following compositions: #1, 0 B; #2 0.01 B, #3 0.02 B, #4 0.04 B, #5 0.08 B, #6 0.16 B, all in wt fractions.

[c] Angle θ in radians/100 mg.

[d] Numbers in (#) are for second heating.

[e] Only first heatings were made.

[f] Numbers in (#) are for Teflon-coated pans.

[g] First and second heating traces were unusual in appearance and not decipherable.

[h] Av. exotherm about 2/3 as intense as for uncoated pans (see column A).

[i] Spread in values smaller at 40 K/min; almost no effect of Teflon coating at higher heating rate.

Note: The angles given above are intended to emphasize the sense of the slope changes at T_{ll}, T_{exo}, and $T_{l\rho}$, namely, T_{ll} and $T_{l\rho}$ endotherms on first and second heatings; T_{exo}, exothermic on first heating, zero on second heating. Angles were measured with a protractor after drawing construction lines through the midrange of traces [see Fig. 3(A)] to average out "short-time noise" as recommended by W. Hemminger and G. Höhne, Ref. 28, pp. 245ff. Note scale change between 10 and 40 K/min as in Figures 3(A) and 3(B). Above angles are not corrected for scale change. Presence of Teflon did not alter intersection temperatures in any consistent pattern.

Figure 3(A) shows first and second heating traces for the stated conditions, specifically a heating rate of 10 K/min, while Fig. 3(B) shows a first heating trace at 40 K/min. The following comments are pertinent:

1. Figure 3(A) exhibits "short time noise" through which we draw construction lines as recommended by Hemminger and Höhne.[28] The slope changes occurring above T_g are now clearly evident and are designated by the symbols θ_1, θ_2, and θ_3. θ_1 and θ_3 are endothermic corresponding to the T_{ll} and $T_{l\rho}$ transitions. θ_2 is an exothermic resulting from flow plus wetting as explained in connection with eqs. (2)–(4).
2. "Short time noise" is essentially absent for the 40 K/min trace.
3. θ_2 is zero for the second heating trace of Figure 3(A) because the flow and wetting process is complete by the end of the first heating.
4. Table II is a summary of measured angles under conditions stated for Columns A, B, and C, including the use of Teflon-coated pans to minimize wetting of the DSC pans by molten PS.
5. Values of T_{ll} and T_{exo} are plotted in Figure 4 as a function of $\bar{M}_w$ showing T_{ll} independent of $\bar{M}_n$, while T_{exo} is markedly dependent on $\bar{M}_w$, especially above M_c.
6. Table II indicates scatter in the numerical values of θ_1 and θ_2 but the sense remains the same: θ_1 always positive on first and second heatings, but smaller on the later; θ_2 always negative for first heating, zero for second; θ_3 is somewhat erratic in appearance partly, we suggest, because of interference form the forced exotherms, especially at high $\bar{M}_w$.
7. Comparison of Figure 3(B) at 40 K/min with the $\bar{M}_n = 2 \times 10^4$ trace of Figure 1 at 30 K/min shows marked similarity, namely an endothermic peak, as predicted by our postulate of an endothermic slope change caused by T_{ll} becoming dominated at T_{exo} by an exothermic change caused by wetting and flow.

Hot Stage Microscopy

Hot stage microscope observations were conducted on these bimodal blends. It was evident that the starting temperatures for T_{gl} and T_f were only slightly above those for essentially monodisperse specimens. This is consistent with earlier studies by Denny et al.[7,8] However, the T_{gl} and T_f processes were diffuse, occurring over a wide temperature range and showed no decisive end point. This is consistent with the higher values of η_0 which prevailed for blends.

Weighted DSC Pan Lids

An obvious type of experiment was to use a weighted DSC pan lid to facilitate flow and increase the intensity of the exotherm. A few exploratory experiments were conducted using an unsealed hermetic pan with an inverted lid resting on the specimen. The lid was weighted with metallic lead. (Solder based on Pb–Sn eutectic alloys had a T_m process which obscured the polymer traces.) The reference cell contained a weighted lid and an empty pan.

Figure 5 shows a typical trace giving rise to the indicated exotherm with the integrated energy calculated by the 1090 controller-computer. The weighted pan lid is considered analogous to the glass cover slide employed in hot stage microscopy as discussed in Refs. 7 and 8.

Kinetics and Exotherms Associated with Sintering

As noted in Refs. 7 and 8, the coalescence of small particles into one or more large particles is exothermic. Schonhorn et al.[12] used a relationship by Frenkel for the kinetics of sintering in which a key variable is $(\gamma/r_0\eta_0)$ where r_0 is the radius of the two particles which are sintering. The exotherm, discussed by Maeda et al.[29], depends on the surface energy of the material and (R/r), where R is the final radius of the large particle. As noted in Ref. 11, T_{gl} occurs above T_g and below T_{ll} with $\bar{M}_n$ below M_c but above T_{ll} when $M > M_c$. Small particles of low molecular weight should enhance both the kinetics and the magnitude of the exotherm. We do not usually detect an exotherm by DSC with loose powder in the DSC pan. Compacting the powder in a pellet press, especially with very fine powder made by precipitating a dilute solution of PS, can give a noticeable exotherm which interferes with the start of the T_{ll} endotherm. This effect is absent on second heating. Both situations are illustrated in Figure 6. It is possible that the start of the T_{ll} endotherms in the Stadnicki data[1] has been distorted by the sintering process at the several lowest molecular weights.

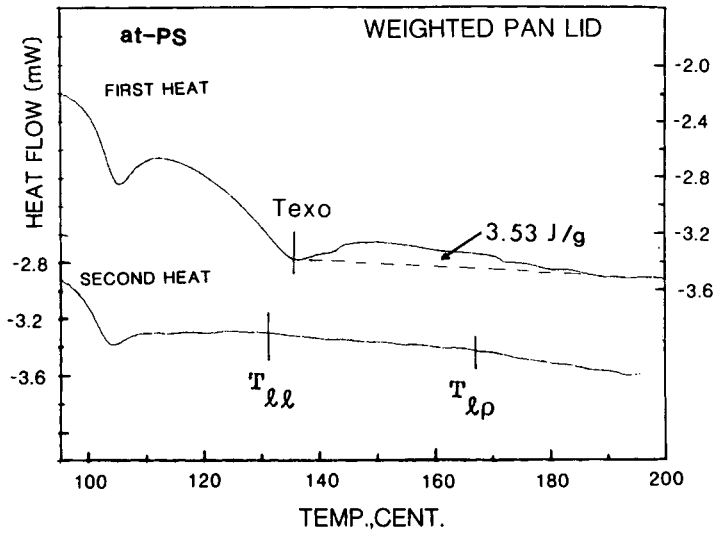

Fig. 5. Weighted pan lid (224.6 mg) with at-PS, $\bar{M}_n$ = 17,500 (8.63 mg), heating rate 10 K min^{-1}. Integrated exotherm is 3.53 J g^{-1}. T_{g1} and T_f from Ref. 7 are 122 and 131° C, respectively. Note sintering exotherm above T_g on first heating only.

In one dramatic DSC experiment for a colleague at MMI, compacted colloidal PS with $r_0 \sim 17$ nm had an exotherm so intense on first heating as to obscure both T_g and T_{ll}. The second heat was normal with a well-defined T_g and T_{ll}. $\bar{M}_n$ of the polymer was 17,500.[30] Dried emulsion PS with $r_0 \sim 170$ nm and $\bar{M}_n$ and $\bar{M}_w \gg M_c$ showed a milder DSC exotherm well above T_{ll} as would be predicted from Figure 1 of Ref. 11.

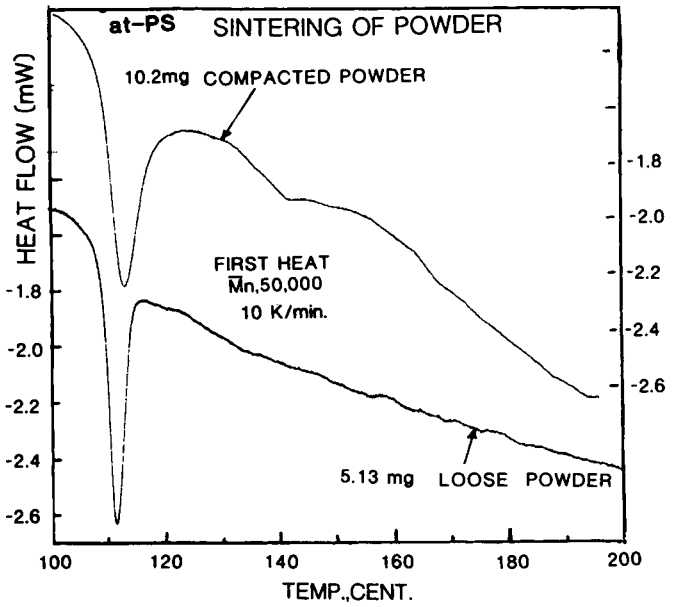

Fig. 6. First heating traces on loose and compacted at-PS powders. T_{g1} and T_f from Ref. 7 are 132 and 147° C, respectively. T_{ll} from Figure 2 is ca. 147° C.

General Remarks about Appendix A

The brief experimental efforts just related were clearly exploratory in nature and designed to illustrate the type of exotherm-based disturbances and their remedies for the liquid state of high T_g polymers. Numerous additional experiments are planned to quantify in greater detail the several types of problems encountered in calorimetry of high T_g polymers. Our original proposition that the apparent DSC endotherm of Stadnicki[1] resulted from competition between a transitional endotherm and a relaxational flow exotherm is now considered substantiated beyond the inferential evidence of Figure 2.

Some comment is in order concerning the maxima in Figure 6 which occur just above the minima in the DSC traces. The classical interpretation of such maxima is based on free volume effects which depend on thermal history.[31] But Figure 6 depicts a situation in which two specimens have the identical thermal history but possess different physical forms and different weights and different thermal conductivities. We suggest, however, that the difference in character of the two hysteresis loops is in part a reflection of the more intense sintering exotherm associated with the compacted specimen, which also has the higher weight of specimen.

APPENDIX B: DSC OF POLY(ALKYL METHACRYLATE)S

Equations (1)–(4) are generic and should apply, for example, to the poly(alkyl methacrylate)s. A study of PMMA ranging in syndiotactic content from ~ 50 to 95% shows a totally different DSC behavior than does at at-PS.[32] In terms of the three angles defined in Figure 3(A), θ_1 appears on first and second heatings as with PS, whereas θ_2 is zero for both heatings. θ_3 is missing but this is likely because T_{l_p} occurs above the top temperatures measured. We explain the DSC behavior of PMMA in Appendix IV of Ref. 32 by noting that η_0 for at-PMMA fractions is at least 100-fold higher than for narrow distribution PSs of the same $\overline{M}_w$ at the same temperature. Flow is greatly reduced with PMMA, and any exotherm is presumably too small to be detected under the experimental conditions employed.

The DSC behavior of P(n-hexyl-MA) from Ref. 22 shows a mild, diffuse maximum in C_p above T_g, similar to those for intermediate molecular weight PSs in Figure 1. P(n-BMA), plotted in Figure 3 of Ref. 11, shows a minimum in C_p (exothermic) starting just above T_{ll} (see also Reference 34).

from monomeric friction coefficients for $\overline{M}_w < M_c$. Ferry[33] gives log monomeric friction coefficients at T_g + 100 K as follows: n-hexyl, −5.18; n-butyl, −4.77; methyl, −3.8; and PS, −6.95.

While the molecular parameters for the several methacrylates just discussed are not as complete as for at-PSs, the observed DSC patterns are understandable when considered in terms of eqs. (1)–(4), and especially the dominant role of η_0.

Note: Reference 32, and especially Appendix IV, seems to emphasize $\overline{M}_n$ values, namely because T_{ll} depends on $\overline{M}_n$. η_0 depends on $\overline{M}_w$, as has been emphasized herein, so that both $\overline{M}_n$ and $\overline{M}_w$ play a role in DSC of the $T > T_g$ region of atactic polymers.

References

1. S. J. Stadnicki, doctoral dissertation, Chemical Engineering Department, Princeton University, 1974.

2. S. J. Stadnicki, J. K. Gillham, and R. F. Boyer, *J. Appl. Polym. Sci.*, **20**, 1245 (1976).

3. J. Chen, C. Kow, L. J. Fetters, and D. J. Plazek, *J. Polym. Sci., Polym. Phys. Ed.*, **20**, 1565 (1982).

4. R. F. Boyer, *J. Polym. Sci., Polym. Phys. Ed.*, **23**, 1 (1985).

5. J. Chen, C. Kow, L. J. Fetters, and D. J. Plazek, *J. Polym. Sci., Polym. Phys. Ed.*, **23**, 13 (1985).

6. R. F. Boyer in *Polymer Yearbook*, R. A. Pethrich, Ed. Harwood Academic, London, 1985, Vol. 2, pp. 233–343 [for an earlier review, see R. F. Boyer, *J. Macromol Sci., Part B, Phys.*, **B18**(3), 461 (1980)].

7. (a) L. R. Denny, K. M. Panichella, and R. F. Boyer, *J. Polym. Sci., Polym. Symp.* **71**, 39 (1984); (b) Errata, *Polym. Lett.*, **23** (May), 267 (1985).

8. R. F. Boyer, MMI, manuscript in preparation.

9. S. E. Keinath, in *Order in the Amorphous 'State' of Polymers*, S. E. Keinath, R. L. Miller, and J. K. Rieke, Eds., Plenum, New York, (1987).

10. Appendix D of Ref. 6.
11. M. L. Wagers and R. F. Boyer, *Rheol. Acta*, **24**, 232 (1985).
12. H. Schonhorn, H. L. Frisch, and T. K. Kwei, *J. Appl. Phys.*, **37**, 4967 (1966).
13. S. Wu, *Polymer Interface and Adhesion*, Marcel Dekker, New York and Basel, 1982.
14. (a) W. M. Lau and C. M. Burns, *J. Colloid Interface Sci.*, **45**, 295 (1973); (b) *J. Polym. Sci., Polym. Phys. Ed.*, **12**, 431 (1974).
15. (a) D. G. Welygan and D. M. Burns, *J. Adhesion*, **10**, 123 (1979); (b) **11**, 41 (1980); **14**, 129 (1982).
16. N. Rosenzweig and M. Narkis, *Polym. Eng. Sci.*, **21**, 1167 (1981).
17. (a) D. J. Plazek and V. M. O'Rourke, *J. Polym. Sci, A-2*, **9**, 209 (1943); (b) R. F. Boyer, *Eur. Polym. J.*, **17**, 661 (1981).
18. (a) J. B. Enns, R. F. Boyer, and J. K. Gillham, *Polym. Prepr. Am. Chem. Soc.*, **18**(1), 629 (1977); (b) **18**(2), 475 (1977).
19. J. K. Gillham and R. F. Boyer, *J. Macromol. Sci., Part B, Phys.*, **B-13**, 497 (1977), specifically pp. 524–530.
20. J. B. Enns and R. F. Boyer, MMI Symposium No. 17, August 1985, R. L. Miller and J. K. Rieke, Eds., Plenum, New York, 1987, to appear.
21. B. V. Kokta, J. L. Valade, V. Hornif, and K. N. Law, *Thermochem. Acta*, **14**, 71 (1976).
22. J. H. Lai, *J. Appl. Polym. Sci.*, **20**, 1059 (1976).
23. V. Bares and B. Wunderlich, *J. Polym. Sci., Polym. Phys. Ed.*, **11**, 861 (1973).
24. F. E. Karasz, H. E. Bair, and J. M. O'Reilly, *J. Phys. Chem.*, **69**, 2657 (1965).
25. C. A. Glandt, H. K. Toh, J. K. Gillham, and R. F. Boyer, *J. Appl. Polym. Sci.*, **20**, 1277 (1976).
26. S. E. Keinath and R. F. Boyer, *J. Appl. Polym. Sci.*, **28**, 2105 (1983), compare Figures 4 and 6; see also S. E. Keinath and R. F. Boyer, *Society of Plastics Engineers ANTEC*, abstract, 1984, Vol. 30, p. 350, Table II.
27. E. I. du Pont de Nemours and Co., Instrument Products Division, Wilmington, DE, 19898.
28. W. Hemminger and G. Höhne, *Calorimetry—Fundamentals and Practice*, Verkag Chemie, Weinheim, Deerfield Beach, FL, and Basel, 1984, esp. pp. 244ff.
29. S. Maeda, S. Iwabuchi, and M. Shiojiri, *J. Appl. Phys. J.*, **23**, 830 (1984).
30. M. Bheda, masters degree thesis, MMI, 1985, unpublished.
31. B. Wunderlich, D. M. Bodily, and M. H. Kaplan, *J. Appl. Phys.*, **35**, 95 (1964).
32. L. R. Denny, R. F. Boyer, and H.-G. Elias, *J. Macromol. Sci., Part B, Phys.*, **B-25**(3), 227 (1986).
33. J. D. Ferry, *Viscoelastic Properties of Polymers*, 3rd ed., Wiley, New York, 1980, p. 330, Table 12-111.
34. R. Hoffman and W. Knappe, *Kolloid Z. Z. Polym.*, **247**, 763 (1971).

Received July 18, 1986
Accepted July 21, 1986